A Novel Ultrasonic Assisted Synthesis of Few Layered Graphene/SnO₂Nanocomposite and Its Electrochemical Properties

Satish Bykkam[a], Bikshalu Kalagadda[b], Venkateswara Rao Kalagadda[a]*, Niveditha Reddy Barray[a], Shilpa Chakra Chidurala[a]

[a]Nano Electronics Laboratory, Centre for Nano Science and Technology, Institute of Science and Technology, Jawaharlal Nehru Technological University Hyderabad, Telangana State, India.
[b]Department of Electronics & Communication Engineering, Kakatiya University, Warangal, Telangana State, India.

ABSTRACT: In this study, Few Layered Graphene (FLG)/Tin oxide (SnO₂) nanocomposite synthesized by ultrasonic assisted synthesis (UAS) method. The uniformly distributed SnO₂ NanoParticles (NPs) on FLG observed by various characterization techniques like electron microscopy techniques (HR-TEM and FE-SEM) for structure and lattice, phase analysis studied by X-ray diffraction (XRD) and functional groups identified by FTIR. Moreover the electrochemical properties of the FLG/SnO₂ nanocomposite was investigated by cyclic voltammerty. The specific capacitance of the prepared FLG/SnO₂ nanocomposite exhibited superior capacitive performance with high capacitance (365 F/g), excellent cyclic performance as compared with Pure SnO₂ NanoParticles. Therefore, the FLG/SnO₂ nanocomposite conceivably a sustainable electrode material for super capacitor and many more energy repository devices for sustainable technological development.

Keywords: *Few Layered Graphene; FLG/SnO₂ nanocomposite; Ultrasonic; Electrochemical Properties; Cyclic Voltametry;*

1. INTRODUCTION

Graphene is a new carbon based material in the field of nanoscience and technology and its high surface area, electrical conductivity, high flexibility and mechanical strength [1, 2]. It's a single atomic layer of the graphite, each carbon atom bonded with strong covalent bonds. The Potential applications of this unique nanostructure hold novel promises for various industrial and professional fields such as nanoelectronics [3, 4], sensor applications [5, 6], different composite materials [7, 8], energy storage devices [9, 10] and hydrogen storage [11]. More ever many types of graphene based composites, such as graphene/TiO₂, graphene/SnO₂, graphene/Fe₃O₄, graphene/ZnO, and graphene/ZrO₂ have become popular because of their unique electrochemical nature in diversified areas [12-17]. Of all these, the SnO₂ compound is considered as a promising material due to it's high capacitance, maximum thermal stability in the air, cost less production and environmental friendliness. SnO₂ nanocomposite based on graphene material were synthesized by UAS method. In this process, the SnO₂ NPs located on graphene's surface have shown unique symbiotic properties of single elements and their different interactions. The combination of these SnO₂ NPs with graphene sheet highly drives to an advanced approach in order to improve their electronic and electrochemical properties.

In this paper, we use an effective and efficient UAS way to synthesize FLG/SnO₂ nanocomposite. The present synthesis UAS method involves HCl acts as reducing agents to convert FLG/SnO₂ nanocomposite by using the precursors Graphene Oxide (GO) and SnCl₂.2H₂O. A simple chemical method was reported by Kim et al. [18] for the preparation of Graphene/SnO₂ nanocomposite which avoid the agglomeration of SnO₂ NPs. Most of conventional method shows the agglomeration of SnO₂ NPs on Graphene sheet. But the present UAS method, the result shows the formation of FLG/SnO₂ nanocomposite and also avoids the agglomeration, which can overcome problems with the previously reported results from Conventional and Non conventional methods.

UAS method mainly improves dispersion of the material and here by synthesizing the out product. Ultrasonic waves are generated at a high frequency related to the applied

potential. In this cavitation phenomenon plays an important role for beneficial effect of chemical reaction, which depends on the ultrasound waves. These waves are induced in the liquid medium and propagated via alternating compressions and rarefactions and the result generates large numbers of the micro bubbles to get produced and interacted in very short life span to bring out the cavitational effects. The generated bubbles are collapsed in the compression cycle, earlier the molecules of the liquid are separated by sound waves of the rarefaction cycle. These phenomena makes high pressure and temperature with cooling rate conditions generate short lived regions by rapid and violent implosions [19-22]. These localized micro bubbles can act as micro reactors to enhance solute transfer and nucleation rate to intense micro mixing leads to the mechanical energy converted into a useful chemical form for the formation of the nanoparticles [19]. Hence, UAS method was proved to obtain particles within the nano range [19-22]. It is expected that the cavitation can play an immense role to avoid the agglomeration during the synthesis route, the cavitation phenomena can induce the oxidation-reduction and also will be easy to decorate SnO_2 NPs between GO and $SnCl_2.2H_2O$ [23] which can enhance the electrochemical properties.

In this current study reports UAS method involves three steps for the synthesis of FLG/SnO_2 nanocomposite. The first step consists of graphite oxide preparation making use of modified hummer's method [24] with the ultrasonic assisted process. The additional step will be conversion of graphite oxide to graphene oxide by following successive steps for the ultra-sonication. Third step involves the preparation of FLG/SnO_2 nanocomposite was carried out by the USA method in the presence of GO and $SnCl_2.2H_2O$. It has been found that SnO_2 NPs decorated on FLG due to ultra-sonication, which is confirmed by HRTEM analysis and also electrochemical characteristics such as specific capacitance, current density of the prepared nanocomposite were studied in an aqueous electrolyte.

2. EXPERIMENTAL

2.1 Synthesis of Graphene oxide

Preparation of GO has been done, as stated in modified hummer's method using ultra sonication with an Ultrasonic Qsonicasonicator (Model no: Q500, 20 KHz Frequency, 500 W) at 45% amplitude as shown in figure 1. Briefly Concentrated H_2SO_4 (46 ml) was mixed with flakes of graphite (2 g) and $NaNO_3$ (1 g)combined solution.
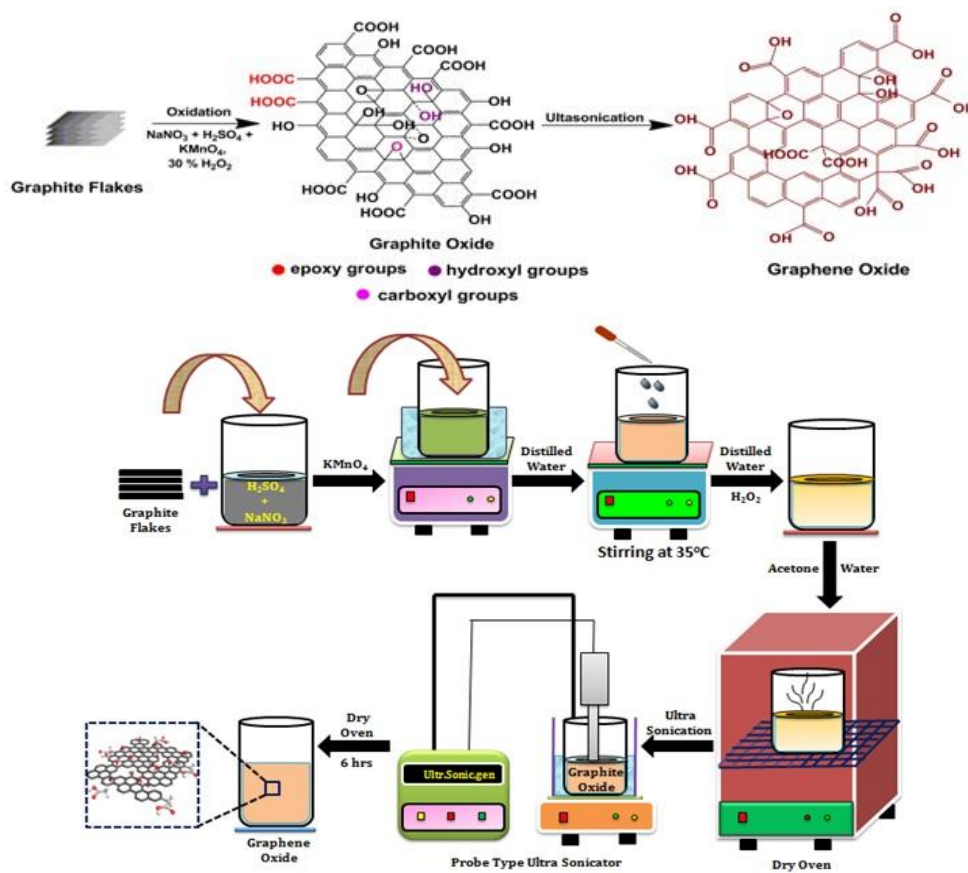

Fig.1: Schematic diagram for the synthesis of graphene oxide.

This prepared solution was kept at low temperature condition surrounding with an ice bath and then drop wise addition of KMnO$_4$ (6 g) to the above mixture , at a reaction temperature of below 20°C while adding KMnO$_4$. Further, the reaction was warmed to 35°C using hot plate with magnetic stirrer for 30min by the addition of (92 ml) distilled water slowly, during oxidation process the color changed from dark purplish-green to dark brown after that the solution was cooled using a water bath for 10 min, additional water (140 ml) was added, with continuation of H$_2$O$_2$(2ml) drop wise addition within the 2min. After this, the color of the solution had changed to bright yellow conforming that the graphite has reached a high oxidation state. The formed solution is subjected to ethanol, 10% HCl solution and DI water wash next to filtration to eliminate metal ions. The acquired was kept for drying in hot air over at 90°C for 12 hours to collect graphite oxide powder (GOP). An 300 mg amount of GOP dissolved in 300 ml of ethanol, kept at a constant stirring rate for 30 min along with 1hour probe type ultra-sonication gives the collective synthesis of graphene oxide. The material formed had gone through

and water wash several times with successive drying for 8 hours in hot air oven to obtain Graphene Oxide (GO).

2.2 Synthesis of FLG/SnO$_2$ nanocomposite

Similar method as above was followed to prepare FLG/SnO$_2$ nanocomposite as shown in figure 2. In this process, 0.5g of GO was mixed with 200 ml of ethanol forming brown color solution through constant stirring for 30 min, and addition of 3ml of ammonia solution to the dispersion solution. Then the mixture was stirred for 60 min at 95°C. Finally an appropriate amount of SnCl$_2$.2H$_2$O and NaOH solution were included into the above GO solution, which was further kept for ultrasonication placed in a 500 ml vessel. The suspension has been through ultrasonication for 2 hours at 35°C proceeding with cooling action at room temperature. The solution acquired is well filtered and washed using distilled water for 3 times, following up with drying in hot air over at 90°C for 5 hours. Calcination of the final output at 600°C for 4 hours in a muffle furnace gave FLG/SnO$_2$ nanocomposite with different weight percentages (FLG; 1.0, 2.0 and 3.0 wt %) by changing the amount of the GO.
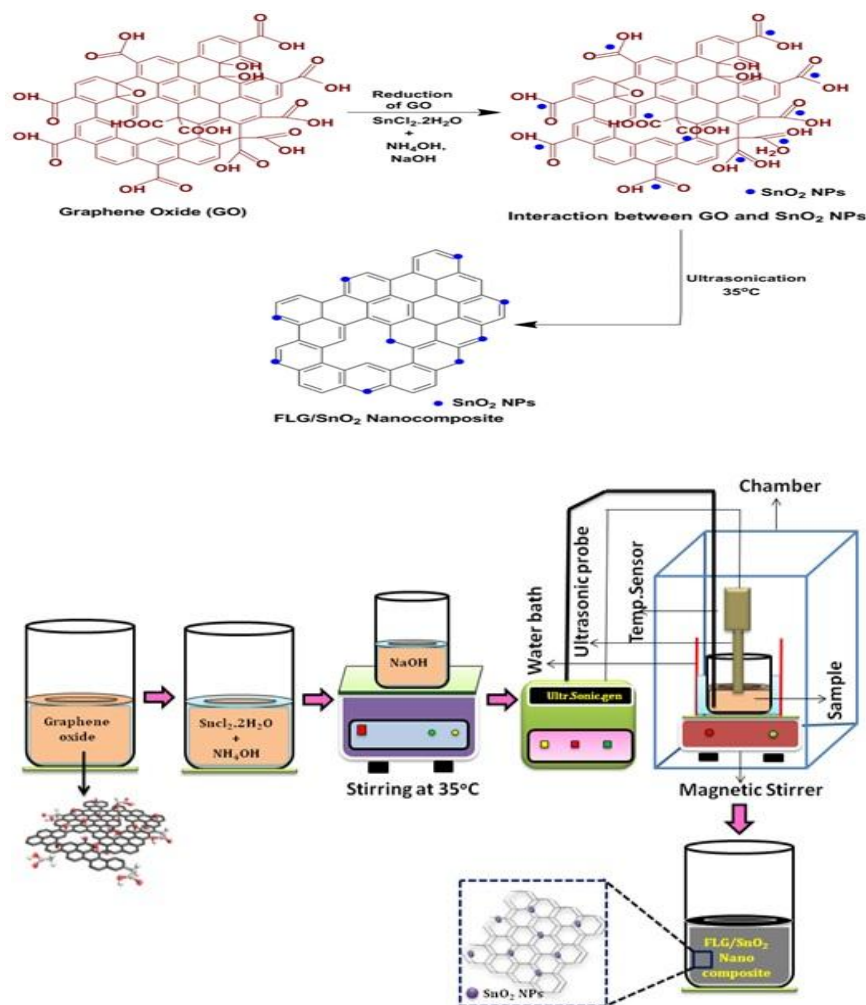

Fig. 2: Schematic diagram of the formation of FLG/SnO$_2$ nanocomposite.

2.3 Characterization

The morphological studies of the sample were analyzed by high resolution transmission electron microscopy (HRTEM, Model no: JEOLJEM 200CX) and field emission scanning electron microscopy (FESEM, Model no: Carl Zeiss Merlin Compact 6027) is opted in order to determine the particle size and decoration of the SnO_2 NPs on the FLG. To know the crystal phase and the composition of the prepared FLG/SnO_2 nanocomposite X-ray diffraction (XRD, Model no: Bruker D8 advanced) with CuKα radiation (k=1.540Å) was used. The presence of different functional groups and formation of graphene in the composite was studied by fourier transform infrared spectrum (FT-IR, Model no: JASCO FTIR-4200) using a standard KBr pellet technique. All electrochemical experiments were performed on a potentiostat (AUTOLAB-PGSTAT 302 N) electrochemical workstation with the three electrode cell system.

2.4 Preparation of working electrode

The fabrication of the working electrodes were done by mixing prepared FLG/SnO_2 nanocomposite (2 mg, 80 wt %), polytetrafluoroethylene (PTFE) binder (10 wt%) and acetylene black (10 wt%). Then the resulting mixture was uniformly grided and punched onto stainless steel mesh (SSM) using a hydraulic press. The FLG/SnO_2 nanocomposite were coated over a stainless steel mesh (SSM) which acts as a working electrode, the counter electrode was chosen as platinum wire and saturated calomel electrode (SCE) to be a reference electrode respectively. The CV measurements were performed in a 6M KOH aqueous electrolyte solution at room temperature. All these three electrodes have been dipped into the supporting electrolyte solution. Bubbling of N_2 gas into the solution for 15 minutes before voltammograms was recorded to remove the dissolved oxygen. The range of the potential window for electrochemical tests were set to -0.6 to -0.3 V. The particular electrode material's specific capacitance can be calculatedby making use of CV curves.

Capacitance can be calculated by making use of CV curves.

$$C_{sp} = \frac{\int Idv}{vmV}$$

(1) Where the specific capacitance of the electrode (F/g) is C_{sp} , response current (A) is I , the potential window (V) is v the mass of the active electrode (g) is m and the scan rate (V/S) is V [25, 26].

3. RESULTS AND DISCUSSION

3.1 Mechanism of GO and FLG/SnO_2 nanocomposite synthesis

The FLG/SnO_2 nanocomposite was prepared by using the UAS method where $SnCl_2.2H_2O$ acts as an agent for oxidation-reduction reaction of GO as shown in (figure 2). The Oxidation mechanism was performed by strong oxidizing agent $KMnO_4$ in the presence of H_2SO_4, in which

graphite flakes are oxidized to form GO and consisting of functional groups attached to them covalently at edges like epoxy, carboxyl, hydroxyl, and carbonyl groups containing oxygen, epoxy and C-OH functional group in different formations attached to each layer of carbon [27]. The reduction reaction mainly removes the oxygen containing groups and enhances the conductivity but there are small residue groups containing on FLG. The hydrolyzation of Sn^{2+} ions is done because of HCL to form SnO_2 NPs with addition of $SnCl_2.2H_2O$ solution to the FLG dispersion, in which Sn^{2+} ions bonded to oxygen atoms of negatively charged residual oxygen containing functional groups on FLG and the addition of NaOH solution generates electrostatic force with relatively high temperature, a large number of Nuclei are formed in a short period of time. These overall reactions were performed by cavitational effects, which makes the oxidation and reduction reaction into a uniform distribution of SnO_2 NPs at room temperature and simultaneously the GO was reduced to FLG.

3.2 HR-TEM analysis

The synthesized FLG/SnO_2 nanocomposite can be confirmed by morphological studies. The characteristic morphology of GO were shown in figure 3(a), the related SAED pattern as shown in figure 3 (b). Figure 3(c) shows that the FLG from GO which is reduced by $SnCl_2.2H_2O$. The tetragonal structures of Pure SnO_2 NPs as shown in Fig 3(d) .Further HR-TEM images show that (Figure 3(e-g)) FLG/SnO_2 nanocomposite with different weight percentages FLG (1.0, 2.0 and 3.0 wt %)/SnO_2.
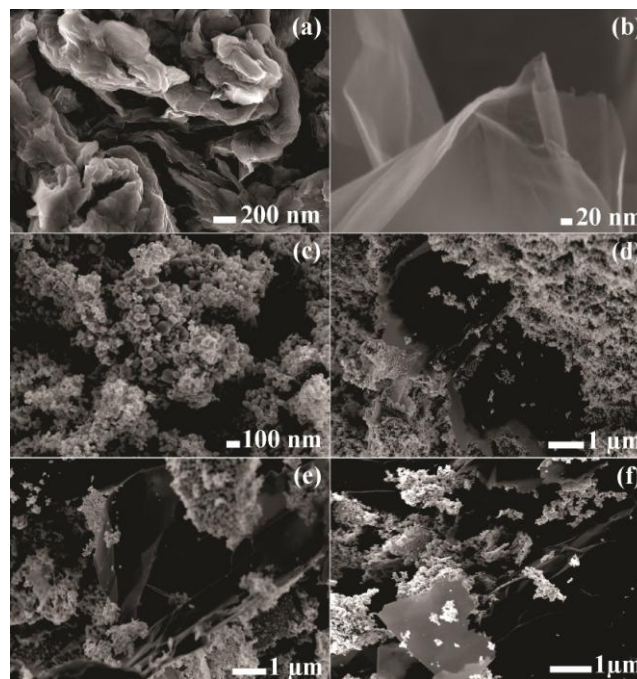

Fig. 3: HRTEM images of (a) GO, (b)SAED pattern of GO (insert)(C) cross sectional image of FLG, (d) SnO_2NPs, (e) FLG(1.0wt%)/SnO_2(f) FLG(2.0wt%)/ SnO_2, (g) FLG(3.0wt%)/SnO_2nano composite.

It is clearly seen that with an increase in the FLG weight percentage in the composite, the SnO_2 NPs were evenly distributed in the form of sand like structures on FLG. This result's observation infers the uniform decoration of SnO_2 NPs, and their high crystallinity and these results got good match with X-ray diffraction (XRD) analysis. Among these three composites, the FLG (1.0 wt %)/SnO_2 has the most suitable structure, in this   a   large number of SnO_2 NPs evenly decorated on FLG.

3.3 FESEEM analysis

Figure 4 (a-c) ascribed the image of the GO, FLG, SnO_2 NPs and Figure 4 (d-f) shows distinguished weight compositions of FLG/SnO_2 nanocomposite FLG (1.0, 2.0 and 3.0 wt %)/SnO_2.The surface morphologyof the GO is observedas anion resemble thetexture which reflects its layer structure (Figure 4(a)) and the ultrasonication process has retained the morphology of the functional groups (Figure 4(b)), the surface area is mostly filled with Pure SnO_2 NPs as shown in Figure 4 (d-f).The FLG may segregate together back to the graphite structure due to the vander walls tendency, decorated with nanoparticles and functional groups which helps in crossing this forbidden action of interaction.
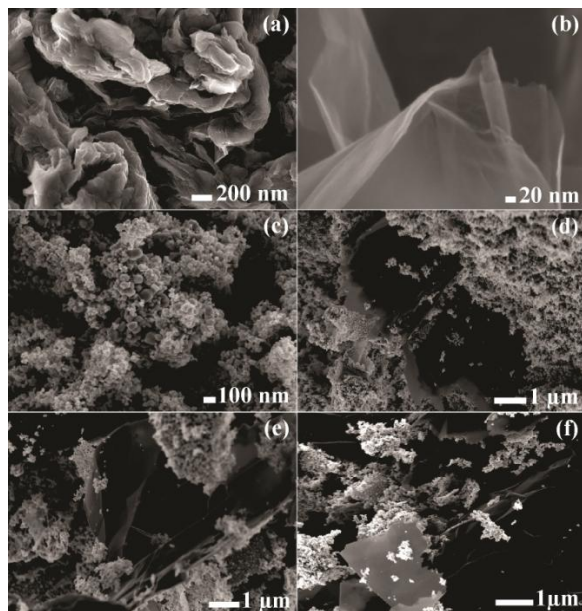

Fig. 4: FESEM images of (a) GO, (b) FLG, (c) SnO_2NPs, (d) FLG (1.0 wt%)/SnO_2, (e) FLG(2.0 wt%)/ SnO_2, (f) FLG(3.0 wt%)/SnO_2 nano composite.

3.4 XRD analysis

The different weight percentages of FLG (1.0, 2.0 and 3.0 wt %)/SnO_2 XRD patterns of GO, FLG, SnO_2 NPs and FLG/SnO_2nanocomposite are shown in Figure 5.The GO's obtrusive diffraction peak was observed at 2θ = 9.09° in correspondence with the plane (001),and having the interlayer spacing (0.87nm).The much higher increase in the value than the graphite (0.34nm)   is observed due to the occupancy of the oxygen obtained functional groups presence on GO and its edges [28]. On the other hand, an
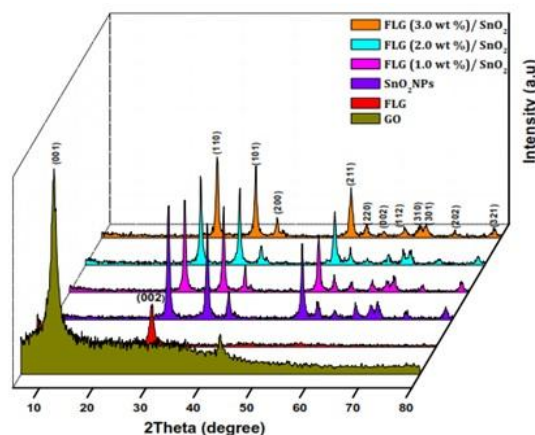

Fig. 5: The XRD pattern of GO, FLG, SnO_2 NPs and FLG(1.0, 2.0 and 3.0 wt%)/SnO_2nano composites.

which indicates FLG, the corresponding plane (002), the inter layer spacing of FLG (0.37nm) is having slight increased variation than the graphite. The obtained diffraction peaks of as synthesized SnO_2 NPs have got good match with standard values (JCPDS card No.41-1445) indicating pure tetragonal phase structures with lattice parameters. The SnO_2 NPs peaks are 26.8, 33.9, 37.9, 51.8, 54.8, 57.7, 61.8, 66.0, 71.2, 78.6° at 2θ and (110), (101), (200), (211), (220), (002), (311), (112), (301), (202), (321) are the correspondence of planes which have shown the tetragonal structures formation respectively. The intensity of the planes decreased compared to SnO_2 NPs, when increasing the weight percentages of FLG in FLG/SnO_2 nanocomposite. Using scherre's equation D = 0.9 λ /βcosθ to calculate, average crystalline size were 25, 23, 21 and 19 for SnO_2 NPs and FLG (1.0, 2.0 and 3.0 wt %)/SnO_2 nanocomposite respectively. Where λ, β are the wavelength of the X-rays, the full width half maximum (FWHM) in radians, and θ is the diffraction angle. The stammer of FLG peak with the (110) peak of SnO_2 NPs (26.8°). In the XRD patterns of the FLG (1.0, 2.0 and 3.0 wt %)/SnO_2 nanocomposite makes it difficult to identify the characteristic (002) peak of FLG at 26.6°.

3.4 FTIR analysis

The further confirmation of the synthesized GO, FLG, SnO_2 and FLG/SnO_2nano composite is done by the FTIR spectra (Figure 6).The IR spectrum of GO(Figure 6(a)), gives the characteristic peak at 3447cm⁻¹ which attributes to O-H stretching bands between absorbed water (H_2O) molecules and structural OH groups, the characteristic peak at 1733cm⁻¹ is corresponded to the GO stretching band of C=O stretching vibration of –COOH groups situated to its edge, the peak at 1641cm⁻¹ is attributed to O-H vibrational bendings. The C-OH functional groups presence, C-O-C vibrational streching can also be detected at peaks around 1384cm⁻¹ and 1123cm⁻¹. It is observed, there is a prominent decrease in the peaks of carboxyl group and also an evolving peak was observed at 1653cm⁻¹ appears in the

spectrum, the corresponding to the skeletal vibration of FLG (Fig 6 (b)) [29].
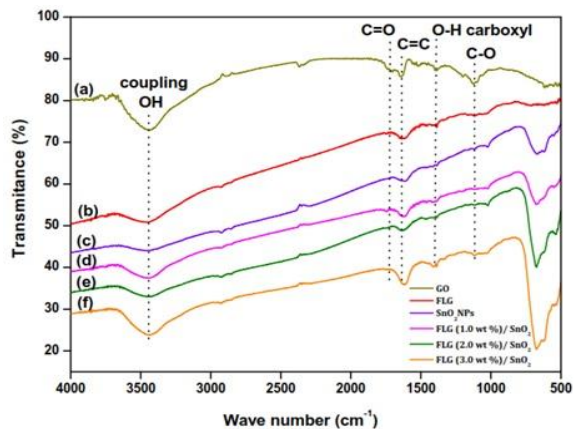

Fig. 6: FT IR transmittance spectra of (a) GO, (b) FLG, (c) SnO₂NPs, (d)FLG(1.0 wt%)/SnO₂, (e) FLG(2.0 wt%)/ SnO₂, (f) FLG(3.0 wt%)/SnO₂nanocomposite.

The FTIR results reveal that Sn^{2+} takes the oxygen of the carboxyl group to be SnO_2 carbolic groups of GO loose oxygen atom and then are reduced to the carbon skeleton of graphene [30]. These shows GO has been reduced by Sn^{+2} during the sonication process. In additional (Figure 4(c)) the characteristic peaks at 668cm^{-1} because of the vibrations of Sn-O and the stretching modes of O-Sn-O, in specific. The potential peak of 668cm^{-1} is designated to (Sn-O-Sn) tin oxide's vibration [31-32], which confirms the occurrence of SnO_2 NPs in the composite prepared (Figure d-f).The C-O at ~1085cm^{-1} and O-H at 1335cm^{-1} are the peaks of FLG/SnO_2 nanocomposite were certainly depleted. The Sn^{+2} of the composite was oxidized to Sn^{+4}, finally transformed functional groups, SnO_2 NPs decorated on the surface of the FLG to form a sandwich structures as mentioned above (Figure 3 (f)). The special open structure of FLG makes easy arrival of electrolyte ions at the interior of the composite, which results the enhanced electrochemical properties.

3.5 Electrochemical properties

Fig 7(a) represents the multiple weight ratios of FLG (1.0, 2.0 and 3.0 wt %)/SnO_2 nanocomposite's CV curves of GO, FLG, SnO_2 NPs at a scanning speed of 10 mV/S with a possible range of -0.6 to -0.3 V in 6 M KOH solution used as electrolyte. In our experiment, the shapes of CV cycles are quasi-rectangular with redox peaks along with the current-potential direction of all the samples has a good capacitive behaviour in super capacitor. The current values of CVs for FLG (1.0 wt %)/SnO_2 nanocomposite electrode were higher than the GO, FLG, SnO_2 NPs and other FLG(2.0 and 3.0 wt%)/SnO_2 nanocomposite. In Figure 7(b) gives the CV curves of FLG (1.0wt %)/SnO_2 nanocomposite at scan rate of 5 to 40 mV/S. The rise of scan speed, results in similar quasi-rectangular shapes of the FLG (1.0 wt%)/SnO_2 nanocomposite. This hybrid structure FLG (1.0 wt %)/SnO_2 results the beneficial to the cation diffusion and also enhance the electrochemical properties.

Among these CV curves (Fig 7(a)), the CV area of FLG (1.0 wt%)/SnO_2nanocomposite is the highest, which means this composite has high accessibility of electrolyte ions due to the largest specific capacitance.
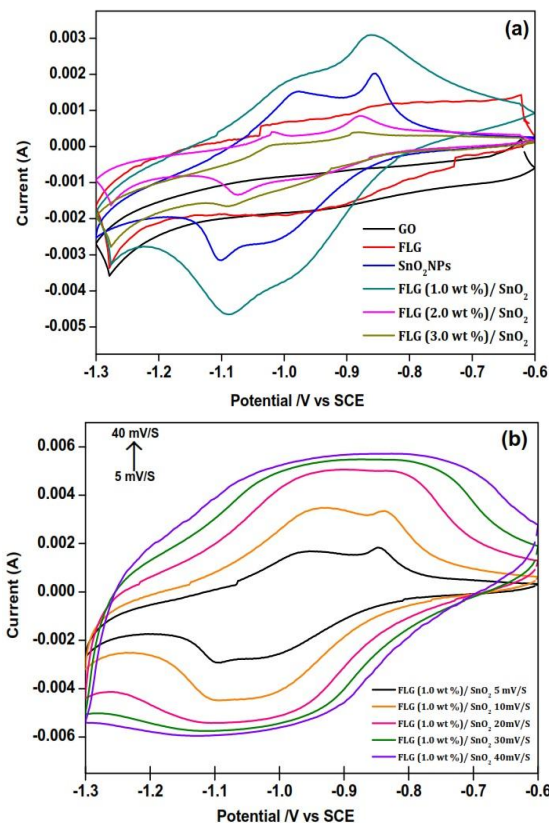

Fig. 7: (a).CV curves of GO, FLG, SnO_2 NPs, and diversifies weight compositions of FLG (1.0, 2.0 and 3.0 wt%) /SnO_2nanocomposite at a scanning range of 5 mV/S in 6M KOH electrolyte solution. (b) CV curves of FLG (1.0wt %)/SnO_2nano composite at different scan rate (5,10, 20, 30, 40 mV/S) in 6M KOH electrolyte solution.

For this composite, the space between FLG can be enhanced by fine and uniform decorating SnO_2 NPs, which obviously makes electrolyte ions, are easy to access inside of the composite. This configuration was supported by the observation of HR-TEM Image are also shown in Figure 3 (f). In the case of the FLG (2.0 wt %)/SnO_2 nanocomposite are few SnO_2 NPs are decorated on the surface of the FLG (which can be seen from Figure 3(g) HRTEM) so that the volume change of FLG cannot be made fully accessible for exchange of electrolyte ions, and the pseudo capacitance functionality of SnO_2 NPs couldn't achieve appropriate results. The exceptional rise in the weight composition of FLG (3.0 wt %)/SnO_2 nanocomposite, has lead to more volume occupancy on the SnO_2 NPs with FLG, where CV results showed that the decrease of electrochemical performance than the FLG (2.0 wt %)/SnO_2, GO, FLG and SnO_2 NPs. The specific capacitance is calculated from the formula (2) for the GO, SnO_2 NPs, FLG and multiple weight percentages of FLG (1.0, 2.0 and 3.0 wt %)/SnO_2 nanocomposite at 5 mV/S as shown in Figure 8(a). From

capacitance was achieved for FLG (1.0 wt %)/SnO₂ nanocomposite than the GO, FLG, SnO₂ NPs and other remaining composites (FLG (2.0 wt %)/SnO₂, FLG(3.0 wt %)/SnO₂).Which was calculated as of FLG(1.0 wt %)/SnO₂ nanocomposite's   higher specific capacitance (C_{sp})value where electrode can reach as high as 365 F/g.
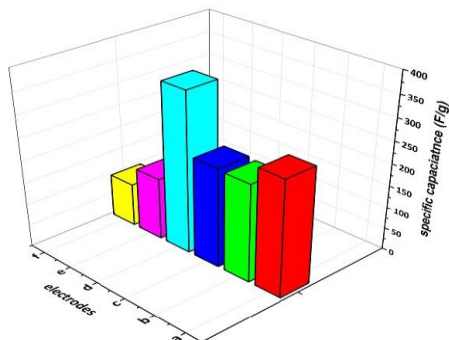

Fig. 8: (a).The specific capacitance of (a)GO, (b)FLG, (C)SnO₂ NPs, (d) FLG(1.0wt)/SnO₂, (e) FLG(2.0 wt)/SnO₂, (d) FLG(3.0 wt)/SnO₂nanocomposite

Among them the specific capacitance is high for FLG (1.0 w t%)/SnO₂na nocomposite due to the easy transfer of electrolyte ions. For this nanocomposite the specific capacitances are performed and calculated at the different scan rate 5, 10, 20, 30 and 40 mV/S (Fig 8 (b))and these corresponding values are 356, 189.2, 150.2, 121.2 and 101.8 F/g respectively.
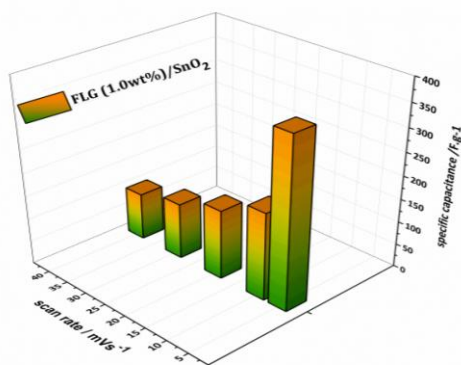

Fig. 8: (b).The specific capacitance of FLG (1.0 wt%)/SnO₂nanocomposite at different scan rates(5,10, 20, 30, 40 mV/S) calculated by CV curves.

This result reflects that the SnO₂ NPs successfully decorated on FLG strongly facilitates enhanced electrochemical properties such as specific capacitance. Therefore, the FLG network, formed by the fine and uniform distribution of SnO₂ NPs, would have acted as active sites for more accumulation of charges. However, an appropriate amount of loading FLG is required in the SnO₂ nanocomposite. On the basis of this result, there is a strong beneficiary effect in the FLG (1.0 wt %)/SnO₂nanocomposite, in which good dispersion of SnO₂ NPs is achieved, presence of FLG improves specific capacitance and superior rate capability in the composite.

4. CONCLUSION

FLG/SnO₂ nanocomposite was successfully prepared through the Ultrasonic assisted synthesis (UAS) method and also GO was reduced to FLG in the presence of HCl and SnCl₂. The cavitational effects occurred by the ultrasonication process creates the oxidation-reduction reaction between GO and SnCl₂.2H₂O, which results in the fine and uniformly decorated SnO₂ NPs on FLG. The surface morphology, crystal phase, chemical binding and electrochemical properties of GO, FLG, SnO₂ NPs and of FLG (1.0, 2.0 and 3.0 wt%) /SnO₂ nanocomposites were investigated. The incorporation of SnO₂ NPs on to FLG and improve the specific capacitance as well as current density. FLG (1.0 wt%)/SnO₂ nanocomposite electrode exhibits the highest capacitance 365 F/g compared with GO, FLG, SnO₂ NPs and other types of FLG (2.0 and 3.0 wt %)/SnO₂ nanocomposite electrodes. This result gives that the FLG (1.0 wt%)/SnO₂ nanocomposite is beneficial for the enhancement of the electrochemical performance, which is considered as a superior electrode material.

REFERENCES

[1] Allen, M. J., Tung, V. C., & Kaner, R. B. (2009). Honeycomb carbon: a review of graphene. *Chemical reviews, 110*(1), 132-145.

[2] Novoselov, K. S., Geim, A. K., Morozov, S. V., Jiang, D., Zhang, Y., Dubonos, S. V., & Firsov, A. A. (2004). Electric field effect in atomically thin carbon films. *Science, 306*(5696), 666-669.

[3] Avouris, P., Chen, Z., & Perebeinos, V. (2007). Carbon-based electronics. *Nature nanotechnology, 2*(10), 605.

[4] Son, Y. W., Cohen, M. L., & Louie, S. G. (2006). Half-metallic graphene nanoribbons. *Nature, 444*(7117), 347.

[5] Schedin, F., Geim, A. K., Morozov, S. V., Hill, E. W., Blake, P., Katsnelson, M. I., & Novoselov, K. S. (2007). Detection of individual gas molecules adsorbed on graphene. *Nature materials, 6*(9), 652.

[6] Sakhaee-Pour, A., Ahmadian, M. T., & Vafai, A. (2008). Potential application of single-layered graphene sheet as strain sensor. *Solid State Communications, 147*(7-8), 336-340.

[7] Stankovich, S., Dikin, D. A., Dommett, G. H., Kohlhaas, K. M., Zimney, E. J., Stach, E. A., & Ruoff, R. S. (2006). Graphene-based composite materials. nature, 442 (7100), 282.

[8] Watcharotone, S., Dikin, D. A., Stankovich, S., Piner, R., Jung, I., Dommett, G. H., ... & Nguyen, S. T. (2007). Graphene–silica composite thin films as transparent conductors. *Nano letters, 7*(7), 1888-1892.

[9] Takamura, T., Endo, K., Fu, L., Wu, Y., Lee, K. J., & Matsumoto, T. (2007). Identification of nano-sized holes by TEM in the graphene layer of graphite and the high rate discharge capability of Li-ion battery anodes. *Electrochimica Acta, 53*(3), 1055-1061.

[10] Wu, Z. S., Parvez, K., Feng, X., & Müllen, K. (2013). Graphene-based in-plane micro-supercapacitors with high power and energy densities. *Nature communications, 4*, 2487.

[11] Novoselov, K. S., Jiang, D., Schedin, F., Booth, T. J., Khotkevich, V. V., Morozov, S. V., & Geim, A. K. (2005). Two-dimensional atomic crystals. *Proceedings of the National Academy of Sciences of the United States of America, 102*(30), 10451-10453.

[12] Wang, X., Zhou, X., Yao, K., Zhang, J., & Liu, Z. (2011). A SnO2/graphene composite as a high stability electrode for lithium ion batteries. *Carbon, 49*(1), 133-139.

[13] Wang, D., Li, X., Chen, J., & Tao, X. (2012). Enhanced photoelectrocatalytic activity of reduced graphene oxide/TiO2 composite films for dye degradation. *Chemical engineering journal, 198*, 547-554.

[14] Kavitha, T., Gopalan, A. I., Lee, K. P., & Park, S. Y. (2012). Glucose sensing, photocatalytic and antibacterial properties of graphene–ZnO nanoparticle hybrids. *Carbon, 50*(8), 2994-3000.

[15] Radhakrishnan, S., Krishnamoorthy, K., Sekar, C., Wilson, J., & Kim, S. J. (2014). A highly sensitive electrochemical sensor for nitrite detection based on Fe2O3 nanoparticles decorated reduced graphene oxide nanosheets. *Applied Catalysis B: Environmental, 148*, 22-28.

[16] Sun, W., Wang, X., Sun, X., Deng, Y., Liu, J., Lei, B., & Sun, Z. (2013). Simultaneous electrochemical determination of guanosine and adenosine with graphene–ZrO2 nanocomposite modified carbon ionic liquid electrode. *Biosensors and Bioelectronics, 44*, 146-151.

[17] Wang, J., Su, M. Y., Qi, J. Q., & Chang, L. Q. (2009). Sensitivity and complex impedance of nanometer zirconia thick film humidity sensors. *Sensors and Actuators B: Chemical, 139*(2), 418-424.

[18] Kim, H., Kim, S. W., Park, Y. U., Gwon, H., Seo, D. H., Kim, Y., & Kang, K. (2010). SnO 2/graphene composite with high lithium storage capability for lithium rechargeable batteries. *Nano Research, 3*(11), 813-821.

[19] Wang, Q., Xia, H., & Zhang, C. (2001). Preparation of polymer/inorganic nanoparticles composites through ultrasonic irradiation. *Journal of Applied Polymer Science, 80*(9), 1478-1488.

[20] Sonawane, S. H., Shirsath, S. R., Khanna, P. K., Pawar, S., Mahajan, C. M., Paithankar, V., ... & Kapadnis, C. V. (2008). An innovative method for effective micro-mixing of CO2 gas during synthesis of nano-calcite crystal using sonochemical carbonization. *Chemical Engineering Journal, 143*(1-3), 308-313.

[21] Mahulkar, A. V., Riedel, C., Gogate, P. R., Neis, U., & Pandit, A. B. (2009). Effect of dissolved gas on efficacy of sonochemical reactors for microbial cell disruption: experimental and numerical analysis. *Ultrasonics sonochemistry, 16*(5), 635-643.

[22] Pinjari, D. V., & Pandit, A. B. (2010). Cavitation milling of natural cellulose to nanofibrils. *Ultrasonics Sonochemistry, 17*(5), 845-852.

[23] Wang, X., Zhou, X., Yao, K., Zhang, J., & Liu, Z. (2011). A SnO2/graphene composite as a high stability electrode for lithium ion batteries. *Carbon, 49*(1), 133-139.

[24] Hummers Jr, W. S., & Offeman, R. E. (1958). Preparation of graphitic oxide. *Journal of the american chemical society, 80*(6), 1339-1339.

[25] Wang, H. W., Hu, Z. A., Chang, Y. Q., Chen, Y. L., Wu, H. Y., Zhang, Z. Y., & Yang, Y. Y. (2011). Design and synthesis of NiCo 2 O 4–reduced graphene oxide composites for high performance supercapacitors. *Journal of Materials Chemistry, 21*(28), 10504-10511.

[26] Wang, W., Hao, Q., Lei, W., Xia, X., & Wang, X. (2012). Graphene/SnO 2/polypyrrole ternary nanocomposites as supercapacitor electrode materials. *RSC Advances, 2*(27), 10268-10274.

[27] Wang, G., Wang, B., Park, J., Yang, J., Shen, X., & Yao, J. (2009). Synthesis of enhanced hydrophilic and hydrophobic graphene oxide nanosheets by a solvothermal method. *carbon, 47*(1), 68-72.

[28] Jin, Y., & Jia, M. (2015). Design and synthesis of nanostructured graphene-SnO2-polyaniline ternary composite and their excellent supercapacitor performance. Colloids and Surfaces A: Physicochemical and Engineering Aspects, 464, 17-25.

[29] Lian, P., Zhu, X., Liang, S., Li, Z., Yang, W., & Wang, H. (2010). Large reversible capacity of high quality graphene sheets as an anode material for lithium-ion batteries. *Electrochimica Acta, 55*(12), 3909-3914.

[30] Li, Z., Shen, W., Zhang, X., Fang, L., & Zu, X. (2008). Controllable growth of SnO2 nanoparticles by citric acid assisted hydrothermal process. *Colloids and Surfaces A: Physicochemical and Engineering Aspects, 327*(1-3), 17-20.

[31] Seema, H., Kemp, K. C., Chandra, V., & Kim, K. S. (2012). Graphene–SnO2 composites for highly efficient photocatalytic degradation of methylene blue under sunlight. *Nanotechnology, 23*(35), 355705.

[32] Tuinstra, F., & Koenig, J. L. (1970). Raman spectrum of graphite. *The Journal of Chemical Physics, 53*(3), 1126-1130.